Numerical modelling of electromagnetically-driven turbulent flows using LES methods

F. Felten, Yves Fautrelle, Y. Du Terrail, Olivier Métais

Numerical modelling of electromagnetically-driven turbulent flows using LES methods

F. Felten [a], Y. Fautrelle [a,*], Y. Du Terrail [a], O. Metais [b]

[a] *Institut National Polytechnique de Grenoble, INPG/ENSHMG/EPM, B.P. 95, 38402 Saint Martin d'Hères Cedex, France*

[b] *Institut National Polytechnique de Grenoble, INPG/ENSHMG/LEGI, B.P. 95, 38402 Saint Martin d'Hères Cedex, France*

Abstract

We deal with the prediction of electromagnetically-driven turbulent flows by means of a large-eddy-simulation method (LES). The model is applied in the case of a liquid metal pool submitted to a polyphase linear electromagnetic stirrer. We investigate two cases: (i) the effects of the pulsating part of the Lorentz forces are neglected, the frequency of the applied magnetic field being high enough; (ii) the oscillating part of the electromagnetic forces is taken into account, the frequency of the magnetic field being sufficiently low. The LES predictions agree well with the mean velocity measurements, as does the standard k–ε model. However, as for the turbulent kinetic energy predictions, there is a large discrepancy between the two models. When the oscillating part of the Lorentz forces is taken into account, the computations show that the fluid flow is sensitive to the unsteady part of the forces provided the frequency of the magnetic field is sufficiently low. The mean velocity is not affected by the fluctuating component of the force. As for the turbulence parameters, the presence of the pulsating part leads to a significant reduction of the turbulent kinetic energy, whilst the turbulence length scale decreases. The effect of the oscillating part of the Lorentz forces becomes negligible when the magnetic field frequency exceeds approximately 5 Hz.

1. Introduction

Electromagnetic stirring is commonly used in various metallurgical processes. In continuous casting for example, it may improve the structure of the solidified metal products. Fluid flows

* Corresponding author.

E-mail address: yves.fautrelle@inpg.fr (Y. Fautrelle).

generated by electromagnetic stirrers have been extensively investigated (see for example, [1]). As for numerical predictions, many works have been published on the subject. In most of the previous works, one-point closure models have been used. The most used model is the well-known k–ε model. Those models yield fairly good results as for the mean velocity prediction. However, it has two main drawbacks:

(i) the turbulence is generally not predicted accurately,
(ii) it is not well fitted for unsteady flows as well as transitional turbulent motions, where the Reynolds number is moderate.

Unsteady behaviours have been reported in aluminium continuous casting, where long period strong temperature fluctuations with long period have been observed [2]. It is likely that those temperature fluctuations are closely linked to flow fluctuations. An other situation concerns electromagnetically-driven turbulent flows. The electromagnetic forces contain a mean part as well as an oscillating one, which generally is of the same order as the mean part. The pulsating forces have never been considered in the various investigations. It is generally admitted that the liquid metal inertia is important, and the liquid metal is not sensitive to the force pulsations. That assumption may be easily justified by simple estimates in the usual cases where the frequency of the applied magnetic field is of order of 50 Hz or more. Nevertheless, the assumption becomes questionable when low frequency electromagnetic stirrers are used. For example, when the magnetic field frequency is of order of a few Hertz, the period of the oscillating part of the forces is comparable to the turnover times of the turbulent structures, as it will be shown later. Thus, neglecting the pulsating part of the Lorentz may be hazardous.

Usual k–ε models are not well fitted to take account of oscillating body forces, and other types of turbulent model must be used. The aim of the present work is to investigate the possible effects of the alternating part of the Lorentz forces on a liquid metal by means of large-eddy-simulation methods (LES). It is also of interest to give some indications on the potentiality of the LES methods in comparison with the standard k–ε models when it is applied to electromagnetically-driven flows.

In the present study, we deal with the prediction of electromagnetically-driven turbulent flows by means of a LES method. The method stems from the Smagorinsky eddy viscosity model. The model is applied in the case where a liquid metal pool is submitted to electromagnetic forces created by polyphase linear electromagnetic stirrers. We investigate two cases:

(i) The frequency of the magnetic field is high enough so that the effects of the pulsating part of the Lorentz forces are neglected (referred hereafter to as Case 1);
(ii) The frequency of the magnetic field is low (a few Hertz), then the oscillating part of the electromagnetic forces is taken into account (referred hereafter to as Case 2).

Case 1 usually corresponds to situations where the magnetic field frequency is high enough, e.g., $f = 50$ Hz. Due to its inertia, the fluid motion is not influenced by the body force oscillations. However, it will be shown later that the influence of the pulsating part of the forces is negligible as soon as the magnetic field frequency is greater than 5 Hz approximately.

In order to test the numerical model, we choose the case identical to that treated by Dubke et al. [3], where mean velocity measurements are available.

2. The numerical model

2.1. The LES model

Let us first describe the LES model, we presently use. A survey of the LES methods may be found in [4]. In the LES model, we give up the ambition to yield a deterministic prediction the flow characteristics whose scales are smaller than the mesh size. We only are interested in predicting the three-dimensional flow field at a scale larger than the mesh size. Therefore, the instantaneous velocity field U_i is split into two parts:

- a large scale averaged part $\bar{u}_i$, also called the filtered field, which is calculated,
- a sub-grid part $\bar{u}_i'$, which is modelised.

We introduce the above decomposition in the instantaneous Navier–Stokes equations and achieve the average over a mesh. We then obtain the so-called filtered equations governing the filtered velocity field $\bar{u}_i$, namely

$$\rho \frac{\partial \bar{u}_i}{\partial t} + \rho \frac{\partial}{\partial x_j}(\bar{u}_i \bar{u}_j) = -\frac{\partial \bar{p}}{\partial x_i} + \rho \nu \frac{\partial^2 \bar{u}_i}{\partial x_j \partial x_j} + \frac{\partial T_{ij}}{\partial x_j} + F_i, \tag{1}$$

$$\frac{\partial \bar{u}_i}{\partial x_i} = 0, \tag{2}$$

where ρ, ν, $\bar{p}$, F_i respectively denote the fluid density, the molecular kinematic viscosity, the filtered pressure and the electromagnetic body force. T_{ij} denotes the sub-grid tensor, whose definition is:

$$T_{ij} = \rho \bar{u}_i \bar{u}_j - \rho \overline{U_i U_j}.$$

The sub-grid tensor accounts for the averaged sub-grid part of the velocity field. Closure of the model requires a modelling of that tensor. To that purpose, the simplest LES method consists in using the Smagorinsky model, which introduces a sub-grid viscosity ν_s in the following way:

$$T_{ij} - \frac{1}{3} T_{kk} \delta_{ij} = 2 \nu_s \overline{S}_{ij} \tag{3}$$

with

$$\nu_s = (C_s \Delta)^2 |\overline{S}| \quad \text{and} \quad \overline{S}_{ij} = \frac{1}{2} \left(\frac{\partial \bar{u}_i}{\partial x_j} + \frac{\partial \bar{u}_j}{\partial x_i} \right), \quad \Delta = (\Delta_x \Delta_y \Delta_z)^{\frac{1}{3}}, \tag{4}$$

where Δ_i and C_s respectively denote the mesh size along the i-axis and the Smagorinsky constant. $\overline{S}$ is the second invariant of the shear rate tensor. In principle, the Smagorinsky constant is related to the Kolmogorov constant C_K in the following way [4]:

Table 1
References of the various calculations

	Mesh reference	
	$N1$	$N2$
Number of grid points	6048	20 475
Mesh size (mm)	7.1	4.7
Time steps (s)		
Without the pulsating force part (Case 1)	0.05	0.05
With the pulsating force part (Case 2)	0.02	0.02

$$C_s \approx \frac{1}{\pi}\left(\frac{3}{2}C_K\right)^{\frac{3}{4}} = 0.17, \quad \text{with } C_K \approx 1.5. \tag{5}$$

However, it turns out that in practice C_s has to be adjusted at a value lower than the theoretical value given by (5) in order to minimize the diffusion effects of the sub-grid tensor. The later effect is particularly important near the walls. Therefore, the Van Driest model is used to adjust the value of the Smagorinsky constant in the following way:

$$C_s = C_{s0}(1 - e^{-y^+/A^+}), \tag{6}$$

where y^+ stands for the distance from the wall divided by the viscous sub-layer depth. The friction velocity is determined by means of the classical wall functions in which the instantaneous velocity is used instead of the mean one. The empirical constant $A^+ = 25.0$ is the Van Driest constant, and C_{s0} is chosen to be equal to 0.1.

2.2. The Navier–Stokes solver

The equations have been solved by means of a finite volume method. The mesh sizes Δ_i are constant and almost equal in the three space dimensions. As for the space derivatives the numerical scheme is a centred second order one. That choice minimizes any numerical diffusion effect in the convective terms discretization. A second order Crank–Nicolson semi-implicit scheme is used for the time dependence. The time step and the mesh sizes are chosen in such a way that the Courant number be at most of order of one. Various grids have been tested. The details are given in Table 1. Calculations have been achieved both without and with the pulsating part of the electromagnetic forces (respectively referred to as Case 1 and Case 2). Large computation times are required. For example, in the case where the $N2$-mesh is used, the computation time is approximately 10^4 mn on a SUN-Sparc workstation.

3. The geometry and the electromagnetic forces

In order to test the model, we use the experimental results obtained by Dubke et al. on a cold mercury simulation [3]. They achieved mean velocity measurements in a parallelepipedic pool located between two linear horizontal electromagnetic stirrers. The geometry as well as the dimensions are shown in Fig. 1.

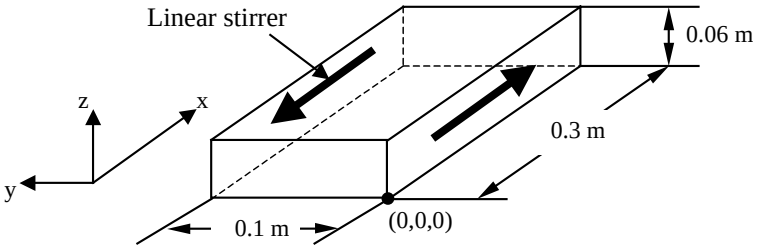

Fig. 1. Scheme of the geometry.

Using the forces calculations derived by Dubke et al. [3], the rotational part of the electromagnetic forces is oriented along the x-axis. For example, in the case of a single stirrer its analytical expression is:

$$F_x = F_0 \mathrm{e}^{-2\alpha y}(1 + \cos(2\omega t - 2\lambda x - 2\beta y)), \tag{7}$$

where

$$F_0 = \frac{\sigma\omega}{2\lambda} B_0^2$$

and $B_0 =$ applied magnetic field strength, $f =$ frequency of the electromagnetic field, $\omega = 2\pi f =$ pulsation, $\sigma =$ electrical conductivity of the liquid metal, $\tau = \pi/\lambda =$ pole pitch, $\mu =$ magnetic permeability, α and β are given by the following formulas:

$$\alpha = \Re\mathrm{e}\left(\sqrt{\mathrm{i}\mu\sigma\omega + \lambda^2}\right) \quad \text{and} \quad \beta = \Im\mathrm{m}\left(\sqrt{\mathrm{i}\mu\sigma\omega + \lambda^2}\right), \tag{8}$$

i being the complex number $\mathrm{i}^2 = -1$.

The ratio $\frac{1}{\alpha}$ is identified to the electromagnetic skin depth.

We consider two different cases corresponding to two magnetic field frequency range:

(i) Case 1, the influence of the oscillating part of the forces is not taken into account,
(ii) Case 2, the oscillatory part of the body forces is kept in the expression (7).

In the experiments, the value of the pole pitch is 0.06 m. Thus, in both cases, the value of the skin depth $1/\alpha$ is imposed mainly by the pole pitch and not by the frequency. Therefore, from (8) the value of α is approximately equal to that of λ:

$$\alpha \approx \lambda = 52.4 \text{ m}^{-1}.$$

In the experimental conditions of Dubke et al. [3], it was checked that (7) was a good approximation of the electromagnetic forces provided an adjustment of F_0. From the force measurements, the fitted value of F_0 is equal to 9220 N/m^3. When two stirrers are used, the force is obtained from (7) by superposition of the forces corresponding to each stirrer. The back influence of the motion on the electromagnetic forces is neglected, although that effect may be non negligible in Case 2.

4. Results

4.1. Averaging procedure

The velocity field, which is initialised to zero, is computed step by step during a time interval of 70 s approximately. Then, the mean velocity field as well as the RMS of the fluctuations are extracted from the numerical data by achieving the time average of the instantaneous values over a significant time interval (60–70 s). We show in Fig. 2 a typical instantaneous value of one of the velocity components in a given location of the pool. In the first four seconds, we observe a transient regime, during which the velocity signal is regular. The corresponding flow pattern is laminar and exhibits symmetries with respect to the pool symmetry planes. Then, the motion suddenly looses its symmetries, and the velocity begins to fluctuate. It may be observed that the velocity signal exhibits long period fluctuations of order of 5–10 s as well. Thus, the time interval has to be long enough in order to obtain a stabilized time average value.

As an illustration, the instantaneous fluid flow pattern in a median horizontal plane is presented in Fig. 3a. That configuration may be compared with the results given by a standard two-dimensional k–ε model in the same conditions (cf. Fig. 3b).

4.2. Effect of the grid size

In order to test the filtering effect of the numerical model, we have analysed the Fourier energy spectra of the velocity fluctuations for various meshes. Some results are presented in Fig. 4. As expected, the frequency turbulent energy spectrum decays less rapidly as the number of grid points increases. That result gives a clue on the behaviour of the model as for the filtering of the small scales of the motion.

Let us now consider the average quantities such as the mean velocity and the turbulent kinetic energy. Regarding the mean velocities, the values computed by the various meshes, e.g., $N1$ and

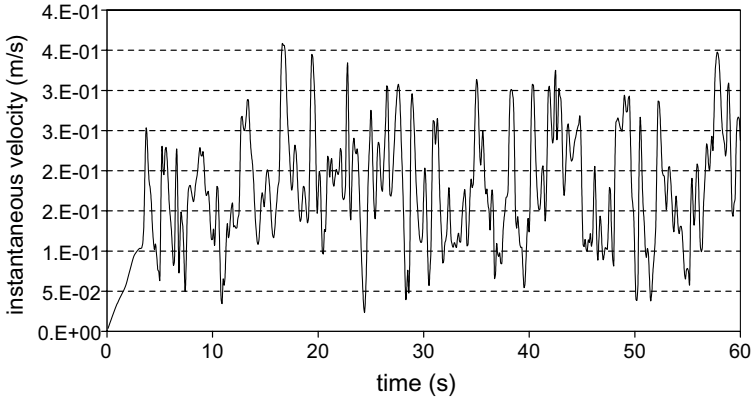

Fig. 2. Instantaneous computed velocity versus time in Case 1 for the intermediate mesh $N2$; the duration of the transient laminar phase is approximately 4 s.

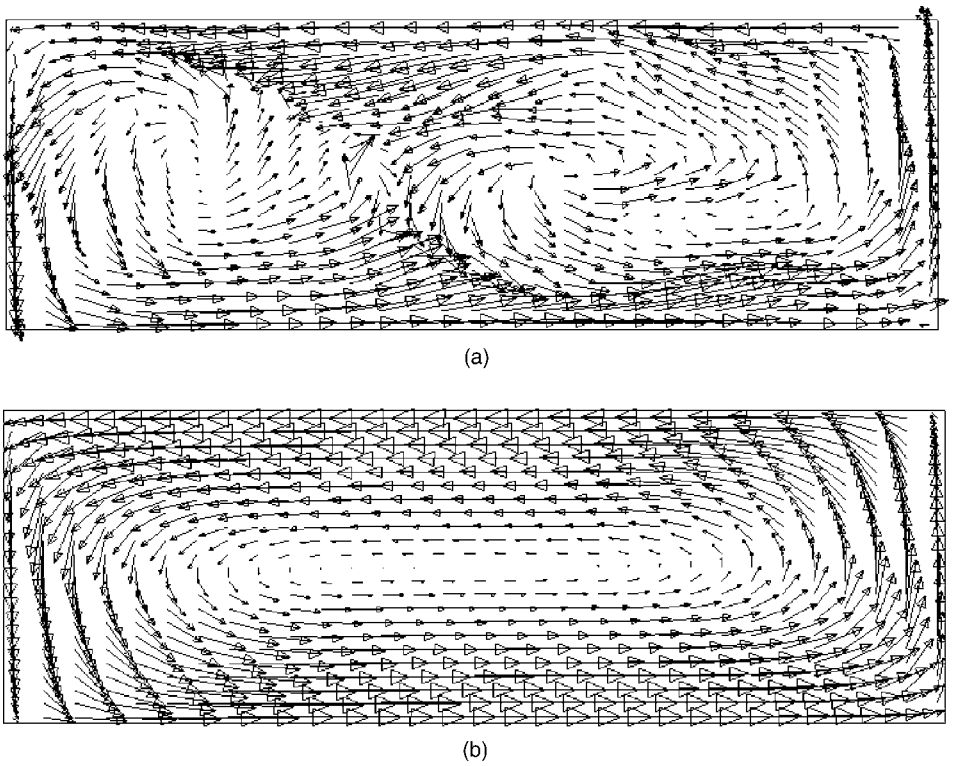

Fig. 3. Flow patterns: (a) instantaneous velocity field computed by the LES method in Case 1 (mesh $N2$) after 20 s from the initial time, (b) mean flow computed by a two-dimensional k–ε model; the view corresponds to a median horizontal plane.

$N2$, are almost identical, and the difference between the profiles is less than 10%. As for the turbulent kinetic energy, the discrepancy is somewhat higher, but it does not exceeds 20%. Thus, the large-scale structures of the flow are not very sensitive to the mesh step or equivalently to the small scales of the flow, provided the mesh step is sufficiently small.

4.3. Comparison with the Kolmogorov theory

The numerical diffusion of the whole model may be also estimated by analysing the behaviour of the computed turbulent energy spectra. Fig. 5 shows a typical frequency energy spectrum $E(f)$, which is converted into a wave number spectrum $E(\eta)$ by means of Taylor's hypothesis. It is of interest to compare the computed spectrum with the theoretical Kolmogorov spectrum, whose expression in the so-called inertial range is [5]:

$$E(\eta) = C_{\mathrm{K}} \varepsilon^{\frac{2}{3}} \eta^{-\frac{5}{3}}, \tag{9}$$

where the turbulent dissipation rate ε is obtained from the computed energy spectrum by the calculation of the following integral:

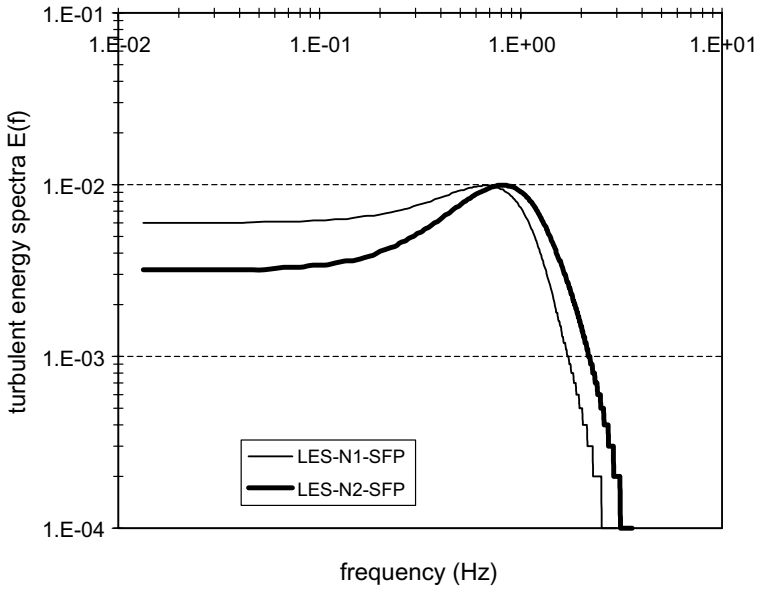

Fig. 4. Computed frequency turbulent energy spectra in Case 1 for two types of mesh: $N1 = 6048$ points and $N2 = 20475$ points.

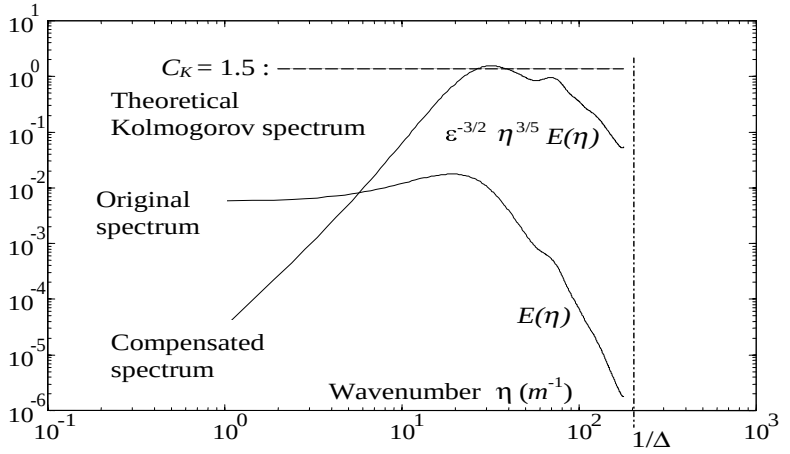

Fig. 5. Computed turbulent energy spectrum in Case 1 (mesh $N2$); the frequency energy spectrum is converted into a wave number spectrum by means of Taylor hypothesis; the straight horizontal dashed line corresponds to the compensated Kolmogorov spectrum given by (9); the straight vertical dashed line corresponds the wave number linked to the mesh size Δ.

$$\varepsilon = 2\nu \int_0^{+\infty} \eta^2 E(\eta)\, \mathrm{d}\eta. \tag{10}$$

The comparison is achieved with the compensated spectrum $\varepsilon^{-\frac{2}{3}}\eta^{\frac{5}{3}}E(\eta)$. We observe that the computed energy spectrum firstly reaches a narrow plateau, which could be interpreted as an

inertial zone as in fully developed turbulence. That range is located in Fig. 5 just before the rapid decay of the compensated spectrum. In principle, the finer the mesh, the wider the inertial zone. That behaviour was more or less illustrated by the spectra of Fig. 4. In our computations, the width of the inertial zone in the turbulent energy spectrum is not very important due to the difficulty to use very fine grids. Nevertheless, it is noticeable that the plateau of the compensated spectrum reaches a numerical value, which is close to the theoretical Kolmogorov constant $C_K \approx 1.5$. That confirms that the observed plateau is actually an (narrow) inertial zone. That result explains why the large-scale motion is not very sensitive to the behaviour of the small-scale structure since a similar phenomenon is observed in fully developed turbulence [5]. Furthermore, the present results indicate that the numerical model is able to yield a fairly good prediction of the largest scale structure of the flow.

After the plateau, the computed spectrum decays rapidly due both to the Smagorinsky viscosity as well as the numerical diffusion. Accordingly, from the spectrum of Fig. 5, we may estimate that the numerical cut-off wave number is of order of $1/(2\Delta)$. The latter result is consistent with our numerical scheme. Therefore, we may conclude that the turbulence structures, whose scale is larger than the cut-off wave number, are quite well predicted. However, as for the smaller turbulence scales, the present LES model cannot yield realistic predictions.

4.4. Case 1: the steady Lorentz forces

Mean velocities. As expected, the mean flow pattern consists of a single horizontal recirculation. The computed mean velocities are compared with the measurements achieved by Dubke et al. [3]. The experimental and computed profiles are shown in Figs. 6 and 7. Those profiles are also compared with the numerical results given by the standard k–ε models both in the three-dimensional and two-dimensional geometries. We observe that the agreements between the various profiles are fairly good. Note that in Fig. 7 the shape of the velocity profile computed with the

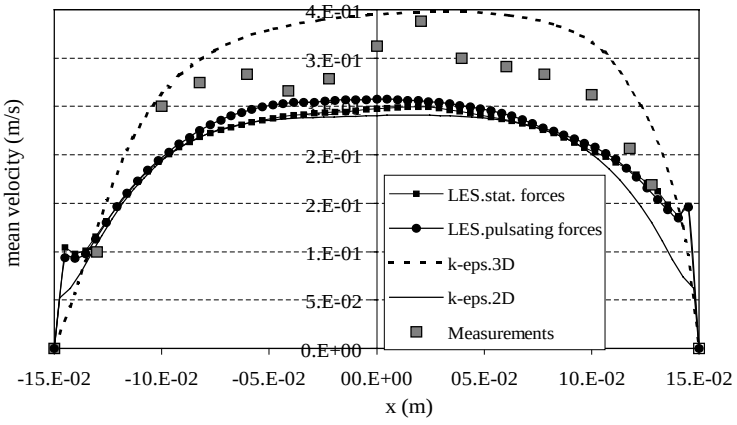

Fig. 6. Comparison between the velocity profiles computed by the k–ε and LES models and the experimental ones (Cases 1 and 2, the mesh reference is $N2$, the magnetic field frequency is $f = 1$ Hz in Case 2); the plot corresponds to the mean y-component along the x-direction in the median plane ($z = 0$) at 1 cm from the wall.

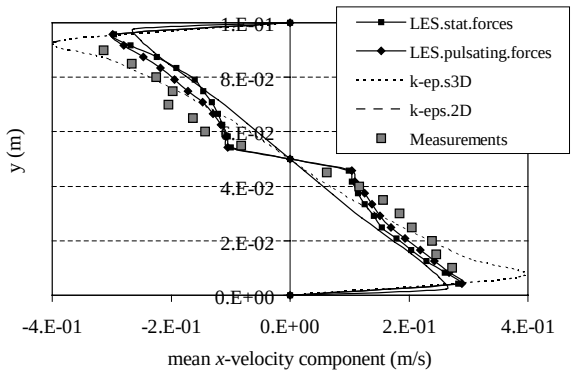

Fig. 7. Comparison between the velocity profiles computed by the k–ε and LES models and the experimental ones (Cases 1 and 2, the mesh reference is $N2$, the magnetic field frequency is $f = 1$ Hz in Case 2); the plot corresponds to the mean x-component along the y-axis in the symmetry planes $(x = 0, z = 0)$.

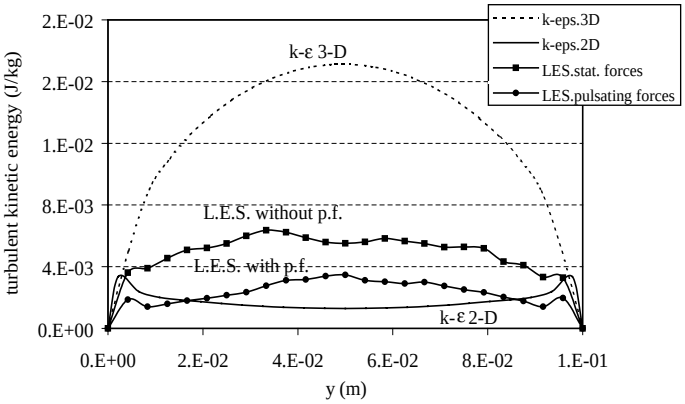

Fig. 8. Turbulent kinetic energy profiles in the symmetry planes $(x = 0, z = 0)$; the velocities are calculated by the LES method without and with the pulsating part of the Lorentz forces (Cases 1 and 2, the mesh reference is $N2$, the magnetic field frequency is $f = 1$ Hz in Case 2); the LES model is compared to with both the 2D and 3D k–ε models.

LES-method seems to be more representative of the experimental data. It is also noticeable that the three-dimensional k–ε model yields quite different predictions.

Turbulent kinetic energy. Since no turbulent kinetic energy measurements are available in that situation, we only compare the computed results given by the k–ε models and the LES model. They are illustrated in Fig. 8. The various turbulent kinetic profiles are not in agreement. Note that there exists a significant difference between the predictions of k given by the three-dimensional and two-dimensional k–ε models themselves. Without any experimental data, it is hard to decide whether the LES predictions are correct or not. We only observe that the turbulence intensity predicted by the LES model is of order of 25%. That value is consistent with turbulence measurements achieved in recirculating flows driven by single-phase electromagnetic stirrers [6]. Note that the prediction given by the three-dimensional k–ε model seems to overestimate the value of the turbulent kinetic energy.

4.5. Case 2: the pulsating Lorentz forces

We now take into account the pulsating part of the Lorentz forces in (7). The computations show that the fluid flow may be sensitive to the unsteady part of the body forces for the lowest frequencies. The influence of the oscillating part is clearly observed for $f = 1$ Hz (cf. Fig. 9), although the amplitude of such oscillations are not really strong at least in the transient phase. The instantaneous velocity field shown in Fig. 9 exhibits oscillations at the frequency of the body forces, i.e., twice the frequency of the magnetic field, especially in the early instant. Those oscillations are no longer visible when the magnetic field frequency f is greater than 4 Hz approximately. Due to inertia, the fluid motion is no longer sensitive to the oscillating part of the forces as soon as $f > 4$ Hz.

Mean velocity. Without any fluid flow measurements available in the low frequency regime, we only are able to compare the cases with and without the oscillating forces. It is found that the mean velocity amplitudes are not really affected by the presence of the fluctuating part of the Lorentz forces. That result is illustrated by the velocity profiles of Fig. 6, where no significant changes are observed between Cases 1 and 2.

Turbulent kinetic energy. The influence of the oscillating part of the Lorentz forces becomes non negligible as soon as the applied magnetic frequency is sufficiently low. From our calculations, the threshold is approximately 5 Hz. In the low frequency regime, we observe from the analysis of the turbulence energy spectrum (cf. Fig. 10) that the typical turbulence time scales are significantly smaller than in Case 1. The maximum of the turbulent energy spectrum, which is shown in Fig. 10, is shifted beyond the frequency of the Lorentz forces, i.e., $2f$ or 2 Hz. That phenomenon is due to the injection of energy by means of the pulsating part of the body force at a scale whose order of magnitude is quite close to the maximum of the spectrum. Let us estimate the typical frequency corresponding to the maximum of the energy spectrum. That frequency is close to $1/\tau_r$, τ_r being the turnover time of the turbulent structure [5]. From Prandtl's theory, the estimate of τ_r is:

$$\tau_r = \mathrm{O}(|\overline{S}|^{-1}), \tag{11}$$

$|\overline{S}|$ being an estimate of the mean velocity gradients already defined in (4).

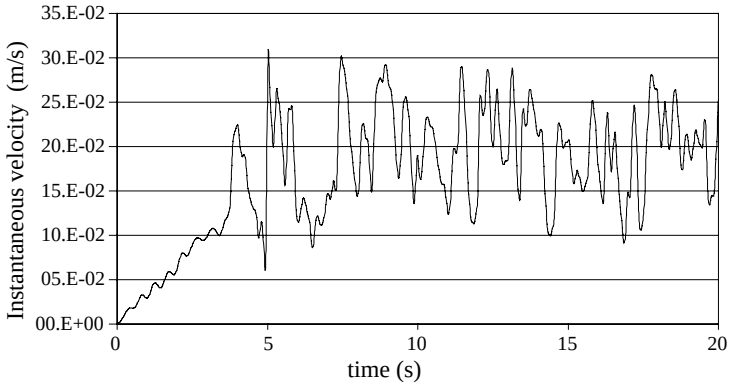

Fig. 9. Instantaneous computed velocity versus time in Case 2 (the mesh reference is $N2$, the magnetic field frequency is $f = 1$ Hz); the duration of the transient laminar part is approximately 4 s; the velocity oscillations at $2f$ are clearly visible during the transient step.

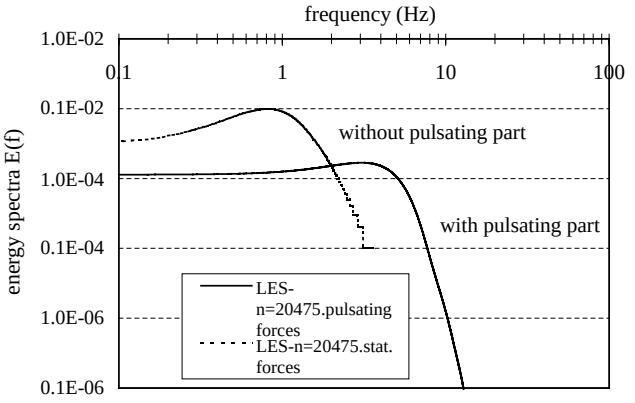

Fig. 10. Computed frequency turbulent energy spectra in Cases 1 and 2; the reference of the mesh is $N2$; the magnetic field frequency for the Case 2 is $f = 1$ Hz; the straight dashed vertical line indicates the frequency of the electromagnetic forces, e.g. 2 Hz; we observe that the spectrum is shifted towards the larger frequencies as expected.

Let $\bar{u}$ and L be respectively the typical mean velocity and the typical dimension of the liquid pool. Let us choose $\bar{u} = 0.2$ m/s and $L = 0.1$ m (width of the liquid pool). Using (11) and the following estimates

$$|\overline{S}| = \mathrm{O}\left(\frac{\bar{u}}{L}\right) \tag{12}$$

yields the value of the turnover time $\tau_r = 0.5$ s (or 2 Hz).

When the magnetic field frequency f is equal to 1 Hz, it is noticeable that the period of the body forces has the same order of magnitude as the turnover time τ_r of the turbulent structure. That last result may explain why and when the turbulent energy spectrum may be modified by the presence of the oscillating part of the body forces. Furthermore, since the mean velocities are almost identical to the previous Case 1, we may also conclude from the Taylor's hypothesis that the turbulence length scales are accordingly smaller.

As for the turbulent kinetic energy, its value is significantly weaker than that obtained in the previous Case 1. This is shown in Fig. 8 (and also in Fig. 10 below), where the various kinetic energy profiles are compared. That result is consistent with the fact that the turbulence length scale l is smaller than in Case 1. Indeed, we may interpret this phenomenon by means of Prandtl's theory, which allows us to estimate the typical turbulent fluctuating velocity $\tilde{u}$ as follows:

$$\tilde{u} = \mathrm{O}(l|\overline{S}|). \tag{13}$$

Since the value of $|\overline{S}|$ remains almost unchanged when the oscillating part of the Lorentz forces is taken into account, the decrease of l implies a correlative decrease of the turbulent velocity fluctuations $\tilde{u}$ and accordingly a decay of the turbulent kinetic energy. Conversely, if the period of the oscillation of the body forces is greater than the turnover time, namely

$$2f\tau_r \approx \frac{2fL}{\bar{u}} \gg 1, \tag{14}$$

then those pulsating forces do not influence the turbulent fluctuations. From a practical point of view, our computations show that the oscillating part of the Lorentz forces is negligible when

$$\frac{2fL}{\bar{u}} \geqslant 5, \tag{15}$$

what corresponds to a magnetic field frequency equal to 5 Hz.

5. Conclusions

We show that the LES model proves to be a good tool in order to predict the large scales of turbulent flows as well as long period unsteady flows. The number of adjustable constants is significantly reduced as compared with the k–ε models. However, the present model has a major drawback, since fine meshes are necessary to accurately predict small turbulent scales. The latter point is particularly crucial near the walls. Very fine grids and accurate numerical schemes are required. Moreover, the present calculations leads to huge computation times, and this actually is the major issue. Despite those drawbacks, the LES model proves to have many potentialities. The mean flow characteristics are fairly well predicted, and it is not necessary to use very fine grids in order to have fairly good predictions. Furthermore, we are able to yield a prediction on the possible effect of the oscillating part of the electromagnetic forces in the low frequency case. According to the model, the pulsating part of the Lorentz forces reduces the turbulent kinetic energy when the magnetic field frequency is of order of a few Hertz. The flow is no longer sensitive to the oscillating part of the Lorentz forces when the applied magnetic field frequency exceeds approximately 5 Hz. From a practical point of view, when low frequency magnetic fields are used, that phenomenon could reduce the efficiency of the stirrer in term of turbulent bulk mixing. Further validations are obviously required.

References

[1] Y. Fautrelle, J. Etay, F. Debray, Stirring and mass transfer in coreless induction furnaces, in: H.Y. Sohn, J.W. Evans, D. Apelian (Eds.), Proceedings of the Julian Szekely Memorial Symposium on Materials Processing, TMS Publication, Warrendale, PA, USA, 1997, pp. 323–338.

[2] J.W. Evans et al., Electromagnetic casting (modelling of heat transport and surface instability), in: Electromagnetic Processing of Materials, Tokyo, The Iron and Steel Institute of Japan, 1994, pp. 160–165.

[3] M. Dubke, K.-H. Tacke, K.-H. Spitzer, K. Schwerdtfeger, Flow fields in electromagnetic stirring of rectangular strands with linear inductors: Part I. Theory and experiments with cold models, Met. Trans. B 19B (1988) 581–593.

[4] M. Lesieur, O. Metais, New trends in large-eddy simulations of turbulence, Annu. Rev. Fluid Mech. 28 (1996) 45–82.

[5] H. Tennekes, J.L. Lumley, A First Course in Turbulence, The MIT Press, London, 1972.

[6] E. Taberlet, Y. Fautrelle, Turbulent stirring in an experimental induction furnace, J. Fluid Mech. 159 (1985) 409–431.